scientific reports

Check for updates

OPEN

Silencing FGL1 promotes prostate cancer cell apoptosis and inhibits EMT progression

Shuaizhi Zhu[1,3,5], Zengshun Kou[1,5], Chengcheng Xiao[2], Lu Wang[2], Jiaxi Zhu[4], Yu Zheng[1] & Hai Zhu[1,2]✉

Emerging evidence from recent studies demonstrates that the FGL1/LAG-3 interaction axis plays a crucial role in mediating tumor immune evasion mechanisms, particularly through the suppression of T lymphocyte effector functions. However, the role of FGL1 in prostate cancer (PCa) remains unclear. Data was downloaded from The Cancer Genome Atlas (TCGA) database, and subjected to differential expression analysis. Single gene differential analysis to determine the correlation between FGL1 and DNAJC12 expression levels in prostate cancer. The expression of FGL1 was silenced by siRNA in PC3 prostate cancer cells. Lentiviruses infected DU145 to overexpress FGL1. Cell proliferation, apoptosis and EMT-related markers were detected in vitro. Animal experiments further confirmed the effect of FGL1 on prostate cancer. Up-regulated gene FGL1 was identified as the selected gene in this study among 3011 Differentially expressed genes. FGL1 had the highest positive relation with DNAJC12. The OS of PCa patients with high expression of FGL1 was significantly shorter. After silencing FGL1, PC3 cell proliferation was inhibited by 0.58-fold, while apoptosis increased by 16%, and the expression of cleaved-caspase-3 increased, while the expression of DNAJC12 and BCL-2 decreased. After overexpression of FGL1, the number of DU145 cells increased by 2.05-fold, the expression of cleaved-caspase-3 was inhibited, E-cadherin expression decreased, while N-cadherin and Vimentin expression increased. Tumor growth was inhibited, and the expression of FN1, n-cadherin, Vimentin and β-catenin decreased, while the expression of E-cadherin increased after silencing FGL1. Silencing FGL1 promotes prostate cancer cell apoptosis and inhibits EMT progression. FGL1 may be an independent prognostic marker and therapeutic target in PCa.

Keywords Fibrinogen-like protein 1 (FGL1), DnaJ heat shock protein family member C12 (DNAJC12), Prostate cancer, Apoptosis, Tumor treatment

Abbreviations

FGL1	Fibrinogen-like protein 1
PCa	Prostate cancer
TCGA	The Cancer Genome Atlas
DEGs	Differentially expressed genes
OS	Overall survival
ROC	Receiver operating characteristic
ADT	Androgen deprivation therapy
CRPC	Castrate-resistant prostate cancer
NSCLC	Non-small cell lung cancer
DNAJC12	DnaJ heat shock protein family member C12
KM	Kaplan–Meier
siRNA	Small interfering RNA
AUC	Area under the curve
RP	Radical prostatectomy

[1]Department of Urology, Qingdao Municipal Hospital, Qingdao University, Qingdao, Shandong Province, China. [2]Department of Urology, Qingdao Municipal Hospital, University of Health and Rehabilitation Sciences, Qingdao, Shandong Province, China. [3]Department of Urology, Qingdao West Coast New Area District Hospital, Qingdao, Shandong Province, China. [4]Life Sciences, Faculty of Arts & Science, University of Toronto - St. George Campus, Toronto, Ontario M5S 1A1, Canada. [5]Shuaizhi Zhu and Zengshun Kou contributed equally to this work and should be regarded as co-first authors. ✉email: shijingzhou@163.com

BCR	Biochemical recurrence
EBRT	External beam radiotherapy

Prostate cancer (PCa) affects millions globally[1]. Prostate cancer (PCa) is the second most common cancer in terms of morbidity and ranks fifth in terms of cancer-associated deaths[2]. Initial management for diagnosed PCa includes radical prostatectomy (RP), radiation therapy, and prostate-specific antigen monitoring for biochemical recurrence (BCR) surveillance. Early-stage PCa patients undergoing RP show favorable outcomes[3]. Multiple steps are involved in the malignant transformation of PCa; it initially presents as prostatic intraepithelial neoplasia, then as localized PCa, later as locally invasive and advanced prostate adenocarcinoma, finally as metastatic PCa, and the interaction between prostate tumor cells and muscle cells surrounding the prostate is considered a risk factor[4]. The 5-year survival rate after early PCa prostatectomy is close to 100%, but metastasis is the primary cause of death[2]. Patients with recurrent PCa and local recurrence after prostatectomy can receive androgen deprivation therapy (ADT) and/or salvage radiotherapy; in contrast, those with systemic recurrence can receive ADT in combination with new androgen signaling-targeted agents or chemotherapy. Advanced PCa usually develops even after ADT is conducted; this type of cancer is recognized to be incurable and castration-resistant[5]. Castrate-resistant prostate cancer (CRPC) refers to PCa progressing during ADT, with serum testosterone levels at the castrate level[6]. Docetaxel-based chemotherapy has delayed CRPC progression for decades[7]. Recent therapies for advanced PCa (cabazitaxel, abiraterone, radium-223, enzalutamide, olaparib, sipuleucel-T, pembrolizumab) target androgen receptor signaling, DNA repair, immune checkpoints, PI3K/AKT, or radiopharmaceutical pathways[8].Despite the good therapeutic efficacy of apalutamide, enzalutamide, and darolutamide against metastatic hormone-naive prostate cancer, multicenter phase III trial data on the effect of these drugs on the overall survival (OS) of patients with CRPC remain limited[9]. We searched public database data to find a new anti-PCa tumor target and verify its role.

Fibroblastibrinogen-like protein 1 (FGL1) has been identified as a functional ligand for lymphocyte-activation gene 3 (LAG-3), a novel immune checkpoint receptor[10]. A 68 kDa protein, whose gene is on human chromosome 8 (8p22–21.3), possesses the disulfide bond-linked homodimer[10,11]. FGL1 is mainly released by hepatocytes in the liver under normal physiological conditions[12]. A meta-analysis from the Oncomine database and TCGA database data showed that it was upregulated not only in the pancreas and liver, but also in prostate and lung cancer samples[12]. In particular, anti-non-small cell lung cancer (NSCLC)--targeted therapy, anti-FGL1, is found to enhance the sensitivity of NSCLC cells to gefitinib[13]. FGL1 silencing enhances the proliferation of LKB1-mutated HCC and lung cancer cells. Besides, FGL1 knockdown elevates tumor cell growth, migration, epithelial-mesenchymal transition, and angiogenesis in A549 lung carcinoma cells with LKB1 overexpression[12]. These factors affect tumor cells via immunity and related mechanisms[13]. There have been a growing number of experiments exploring immunotherapy for prostate cancer, although there has been no clinical breakthrough in immunotherapy[14]. Although related reports indicate that FGL1 is highly expressed in PCa cells, its mechanism remains unclear. We conducted a series of experiments to explore its role in prostate cancer in addition to immunity.

We found a positive correlation between FGL1 and DnaJ heat shock protein family member C12 (DNAJC12) in Pca cells. FGL1 regulates apoptosis through DNAJC12 in Pca, providing a theoretical basis for applying FGL1 for Pca treatment in clinical settings. The present study focused on investigating how FGL1 affects Pca cell apoptosis.

Methods

Data extraction

Gene expression profiles and clinical data of Prostate Adenocarcinoma (PRAD) were obtained from the TCGA database (https://portal.gdc.cancer.gov/). Batch effects were removed from the standardized data and corresponded to relevant clinical samples. Moreover, duplicates were eliminated, samples collected in downloaded data were removed, and patients with insufficient outcome information were excluded. The TCGA database included 481 cancer samples along with 51 healthy subjects. R software v3.6.3 was used for statistical analysis.

Identification of differentially expressed genes

Differentially expressed genes (DEGs) were analyzed by the Limma package of R software (version: 3.40.2). False-positive results were corrected by analyzing adjusted p-values in TCGA. $|\log2(FC)| > 2$ and $P < 0.05$ were selected as the thresholds to select DEGs. Ggplot2 in the R package was used for constructing volcano plots.

Survival analysis

The association of gene expression with OS was evaluated by one-way Cox regression analysis. Using $P < 0.05$, the top five genes were selected. R software was used for one-way Cox survival analysis, and the "Forest map" r package of the forest map was used for result visualization.

Key gene screening

Essential genes were identified by comparing the receiver operating characteristic (ROC) and time–ROC curves of the five genes associated with prostate cancer survival. The relationship between FGL1 expression and survival rate was analyzed using the Kaplan–Meier (KM) approach. To analyze FGL1's role in survival, the "survminer" R package "surv_cutpoint" function was used to determine the best threshold expression level.

Single gene difference analysis
Spearman's correlation was conducted using R software to analyze gene-gene interactions. Further, R software ggplot2 and TIMER2.0 (http://timer.cistrome.org/) were used for visualization.

Analysis of immune infiltrating cells
To evaluate immune infiltration in PRAD, we performed single-sample gene set enrichment analysis (ssGSEA) with the R package GSVA to calculate the relative enrichment scores of 21 immune cell subtypes. The correlation between the expression of five target genes and these immune cells was investigated using Spearman's correlation analysis.

The interaction network analysis
For the biological function of FGL1, we conducted the following analysis. The first 200 genes related to FGL1 in PRAD were obtained from R software. These genes were enriched by Gene Ontology (GO), including biological processes (BP), cellular components (CC), molecular function (MF), and KEGG pathway analyses in the Database for Annotation, Visualization and Integrated Discover (DAVID) and visualized by the R package ggplot2. A corrected $p < 0.05$ was determined to be statistically significant.

Cells and culture conditions
PC3 and DU145 cells were obtained from the Chinese Academy of Sciences (Shanghai, China). LNCaP and 22Rv1 cells were purchased from the American Type Culture Collection (ATCC). Cells were cultured in high-glucose DMEM (SH30022.01B; HyClone, Beijing, China) containing 1% penicillin-streptomycin (3810–74–0; Sigma, USA) and 10% fetal bovine serum (No. F-7524, Sigma, USA) at 37 °C and 5% CO2.

Vector plasmid, psPAX2, and pMD2-VSVG were added to the HEK293T cells with a cell density of 80% and the cells were transfected using the calcium chloride method. The medium was changed 24 h after transfection, and cell supernatants were collected and centrifuged at 48 h and 72 h, respectively. The cells were then screened with 2 μg/mL of Puromycin. Plasmids overexpressing human FGL1 were purchased from Sinobiological (Beijing, China). The calcium transfection kith and Puromycin from Sigma-aldrich.

Transwell migration assay
Cell suspensions (2 × 105 cells/ml) were prepared with serum-free medium. The upper chamber was supplemented with 200ul of suspension cells and the lower chamber with 600ul of complete medium containing 10% FBS. After 24 h in 37 ° C incubator, 4% paraformaldehyde was added and fixed for 30 min. Crystal violet was dyed for 30 min. Take a picture under a microscope. The number of migrated cells counted by IMAGJ software.

RT-qPCR
Total RNA was extracted by TRIZOL method. Reverse transcription PCR (RT-PCR) was performed using EVO M-MLV reverse transcription reagent premix(Accurate Biotechnology(Hunan) Co., Ltd) produced. Next, RT-qPCR was performed using SYBR Green Pro Taq HS(Accurate Biotechnology(Hunan) Co., Ltd) premixed qPCR according to the kit instructions. GAPDH was used as internal control and relative gene expression was normalized by 2-ΔΔCT method.

Small interfering RNA transfection
Small interfering RNAs (siRNAs) were prepared by GenePharma (Shanghai, China). They were transfected into cells to silence FGL1 expression. The sequences of the siRNAs were: FGL1-siRNA, sense, 5′-GGGAAGUUCUA CAAUUCUAAU-3′, and anti-sense, 5′-UAGAAUUGUAGAACUUCCCAG-3′; NC-siRNA, sense, 5′-UUCUC CGAACGUGUCACGUTT-3′, and anti-sense, 5′-ACGUGACACGUUCGGAGAATT-3′. Lipofectamine™ 2000 kit (11668–027; Invitrogen, USA) transfected cells after reaching 30% confluency. The transfected cells were collected for subsequent detection.

Cell viability assay
Stably transfected PC3 cells (2.5×10^4/well) were inoculated into 96-well plates and incubated for 24 h. CCK-8 reagent (10 μL/well, BB-4202–500 T; BestBio, Nanjing, China) was added, and the plates were incubated for another 2 h. Then, the microplate reader (Stat Fax-4200, USA) was used to measure the absorbance (A) value at 450 nm. GraphPad Prism v. 9.0 (GraphPad Software, CA, USA) was used to construct the survival curve, which was used to determine the half-maximal inhibitory concentration.

Ki-67 staining
PC3 cells were fixed with 4% paraformaldehyde, followed by overnight staining with the anti-Ki-67 antibody (cat.no. ab15580, Abcam) at 4 °C and incubation with goat anti-rabbit IgG secondary antibody (cat.no. ab205718, Abcam) for binding to the primary antibody. Cells were photographed using a confocal laser scanning microscope (Olympus Corporation) to detect alterations in nuclear morphologies.

Colony formation assay and wound-healing assay

The transfected cells were seeded in 6-well plates and 2 ml of medium was added to each well. After 12 days of culture, the formation of cell colonies was observed under a microscope. Washes in PBS, fixed in 4% paraformaldehyde for 1 h, then stained in 0.1% crystal violet for 1 h. The relative colony number was counted by Image J. 2×10^6 cells were cultured on 6-well plates. The cell layer was scratched at the confluence using the tip of a 200 μl pipette, and the cells grew under normal conditions. Wound photographs adjacent to the reference

line scratched at the bottom of the plate were taken with a microscope (100 ×) and wound healing was measured at 0 and 24 H.

Apoptosis detection via flow cytometry

PC3 cells were washed twice with pre-cooled PBS, and apoptosis was measured using the Annexin V-FITC Apoptosis Detection Kit (AO2001-029-G, Sungene Biotech, Tianjin, China) according to the manufacturer's protocol. All analyses were performed on a BD AriaIII flow cytometer (BD Biosciences).

Western blotting

Stably transfected PC3 cells (3×10^5/well) were inoculated into 6-well plates and incubated for 48 h. Then, RIPA buffer containing 1% PMSF was added to lyse the cells. Protein content was analyzed using the BCA protein kit (PC0020; Beijing Solabo). After separation by 10% SDS-PAGE, proteins were transferred onto PVDF membranes (ISEQ00010; Milli-pore, USA), followed by specific antibody incubation, including FGL1 (ab197357, Abcam), DNAJC12 (ab254762, Abcam), Bcl-2(ab32124, Abcam) and cleaved-caspase 3 (ab32042; Abcam). Later, membranes were incubated with HRP-labeled secondary antibodies, and protein bands were detected using the chemiluminescent gel imaging system (Clinx Science Instruments Co., Ltd.).

PC3 mouse xenograft model

Twelve male athymic nude mice(GemPharmatech Co., Ltd) aged 6 ~ 8 weeks were randomly divided into two groups, both of which could get enough food and water. The Ethics Committee of the Qingdao University approved this research(QDU-AEC-2024697).All methods were carried out in accordance with relevant guidelines, and were adhered to the ARRIVE guidelines to ensure ethical and methodological rigor. Approximately 1 × 106 PC-3 cells from NC-siRNA and FGL1-siRNA groups were re-suspended in 100μL Matrigel (BD Biosciences) and PBS mixture (1:1) and subcutaneously inoculated into the flank of mice. Subcutaneous tumor formation was observed and recorded weekly. The mice were killed 4 weeks after subcutaneous injection. Anesthesia was inhaled preoperatively with 1% isoflurane (Shanghai Yuyan Instruments Co., Ltd.). Mice were euthanized with excessive isoflurane after operation. Xenografts were collected to measure tumor size. One part of the tumors was detected by immunohistochemistry. The tumor volume was calculated as (width2 × length)/2.

Immunohistochemical: the expression levels of E-cadherin, n-cadherin, Vimentin, β-catenin and FN1 were detected by immunohistochemistry. The sections for staining were obtained from the transplanted tumor tissue of the surgical nude mice. SP-9000 histidine addition kit, 3–3′-diaminobenzidine tetrachloride (DAB) kit, E-cadherin Mouse Monoclonal Antibody, n Cadherin Antibody and Anti-Vimentin, anti-beta-Catenin Antibody and Anti-FN1 Mouse Monoclonal Antibody were used for staining. IHC-stained sections were independently assessed by two pathologists, deciding that any differences in outcome were resolved by consensus.

Statistical analysis

Data were analyzed using SPSS (IBM, USA) and GraphPad Prism (GraphPad Software, CA, USA). Two groups were compared using the Student's t-test. Abnormally distributed data were compared using the Mann–Whitney U test. ROC curves were analyzed using the R version 3.6.3 pROC package to determine the area under the curve (AUC). The KM method was used to analyze patient survival. Univariate and multivariate Cox regression analyses were conducted. A P value of < 0.05 indicated statistical significance.

Results

FGL1 expression in pCa cells

Data were obtained from the TCGA database, including 481 tumor samples and 51 normal prostate tissue samples. Patient characteristics are listed in Table S1. DEGs were identified using edgeR of the R package (Table S2). We identified 3011 DEGs (1254 were upregulated and 1757 were downregulated). The results were visualized using a volcano plot (Fig. 1A). The red and blue dots stand for upregulated and downregulated DEGs, respectively. We analyzed prostate tumor data in the TCGA database by R language by comparing gene expression between prostate normal tissues and tumor tissues, and obtained DEGs conditional on $|\log2(FC)| > 2$ and $P < 0.05$, five target genes(*RRM2*, *SLPI*, *FGL1*, *UGT2B4*, and *FCGBP*) were obtained by sequencing the OS results of univariate Cox analysis ($p < 0.05$) (Table 1). For assessing the roles of cancer genes in prediction, ROC curve analysis was performed for 5 target genes, and the results showed that these genes have high diagnostic efficacy in pCa. (Fig. 1B). After literature review, we found that FGL1 may have an important function in cancer immunity, so we teamed up to study this gene in depth[10]. Next, the Wilcoxon rank-sum test was conducted to compare tumor and normal tissues using data from TCGA-PRAD; tumor tissues had higher FGL1 expression than normal tissues (Fig. 1C; Table S3).We further examined the speed changes in the time–ROC curves, FGL1 showed better predictive power over time for pCa. (Fig. 1D). Finally, we explored the expression of FGL1 in different cancers which revealed that FGL1 was upregulated in melanoma, lung, colorectal, brain, and breast cancer samples (Fig. 1E).

Using R software, we calculated the correlations among the 5 genes screened, FGL1 has the highest correlation with UGT2B4 (Fig. 2A). Immune infiltration analysis of PRAD tumor samples was performed by the R software "CIBERSORT" package, and further analysis of the 5 genes screened was performed. The results show that these genes are associated with a variety of immune cells (Fig. 2B,C). In summary, FGL1 is strongly associated with prostate carcinogenesis and may possibly be related to the immune response.

Relationship between FGL1 and OS

To determine FGL1 grouping, the best-truncated expression level was calculated using the "Survminer" R packet "Surv" function($|\log2(FC)| > 2$ and $P < 0.05$). Increased expression levels of FGL1 (hazard ratio [HR],

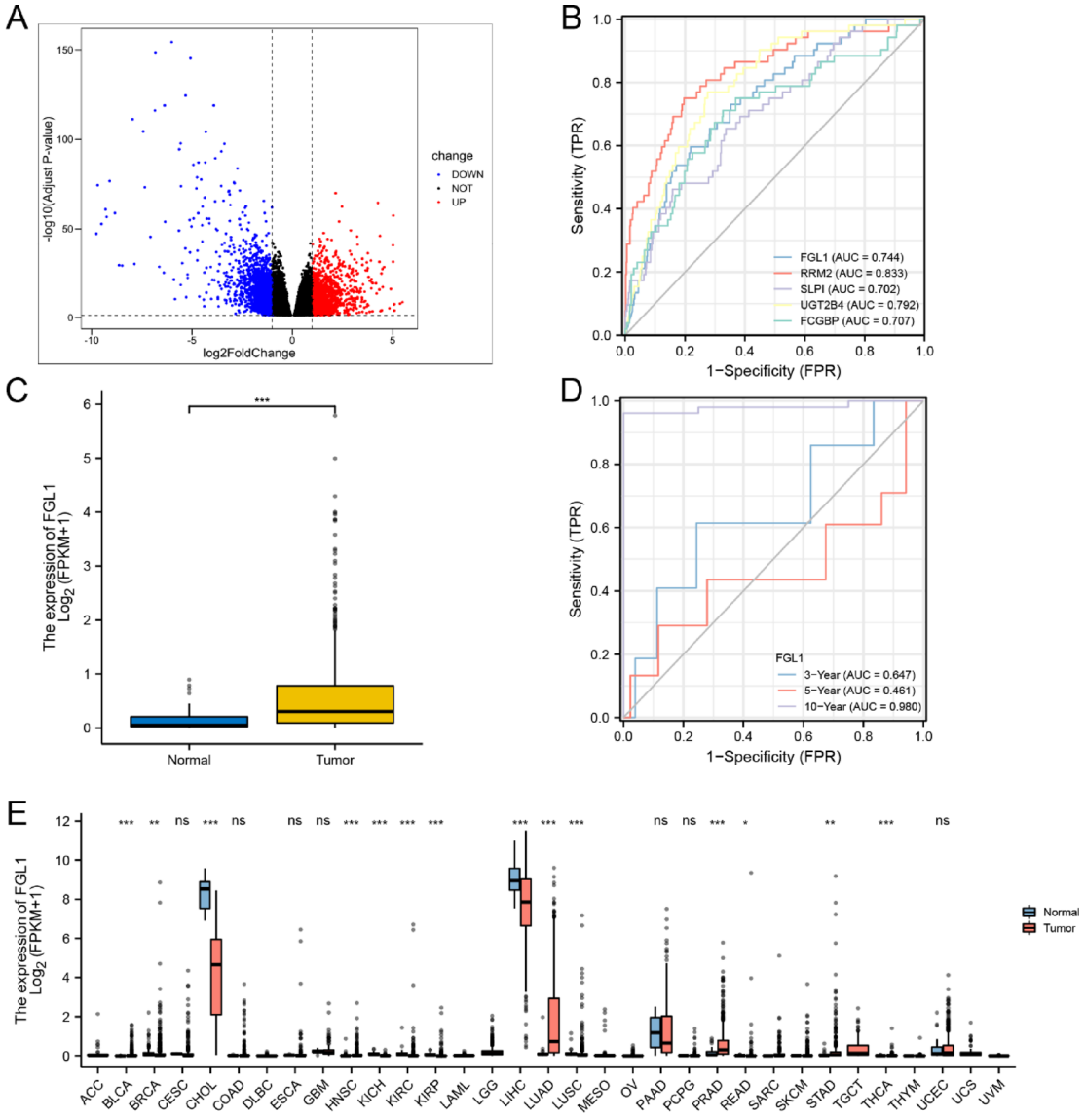

Fig. 1. Differentially expressed genes and Expression of FGL1: (**A**) Volcano plot: red dots indicate significantly differentially up-regulated genes, and blue dots indicate significantly differentially down-regulated genes; (**B**) The ROC curves are shown along with the area under the curve (AUC); (**C**) Expression level of FGL1 in PCa; (**D**) The expression sensitivity of FGL1 was predicted by time receiver operating characteristic (Time-ROC) curve. (**E**) Expression level of FGL1 in 33 cancer types. (ns is $P > 0.05$, * is $P < 0.05$, ** is $P < 0.01$, *** is $P < 0.001$).

5.22; $P = 0.02$) in pCa cells were associated with poor OS (Fig. 3B). High expression of FGL1 correlated with TNM stage. Compared with normal tissues, T2, T3, N0, N1, M0 stages and PSA, age showed significant high expression of FGL1. T4, M1 and PFI were not statistically significant (Figure S3; Table S4–9).

Single gene difference analysis of FGL1 and other genes

We analyzed and visualized the association of FGL1 with other genes using the R software (Fig. 3A). FGL1 had the highest positive correlation with DNAJC12 ($P < 0.001$). Correlation analysis between FGL1 and DNAJC12 was also performed using TIMER2.0 software (Fig. 3C). As FGL1 expression increased in pCa cells, DANJC12 expression also increased.

The interaction network analysis of FGL1-related genes

For the biological function of FGL1, we used R software to enrich the GO function of FGL1-related genes and identify the KEGG pathway. The results of GO enrichment showed that FGL1 and its related genes were related to the growth and development of muscle cells, and biological processes were related to the development and differentiation of muscle cells; cellular components were associated with the development of muscle cells and myosin, the molecular function is suggested to be related to myocytes and some lipid proteins (Fig. 4A,B). KEGG

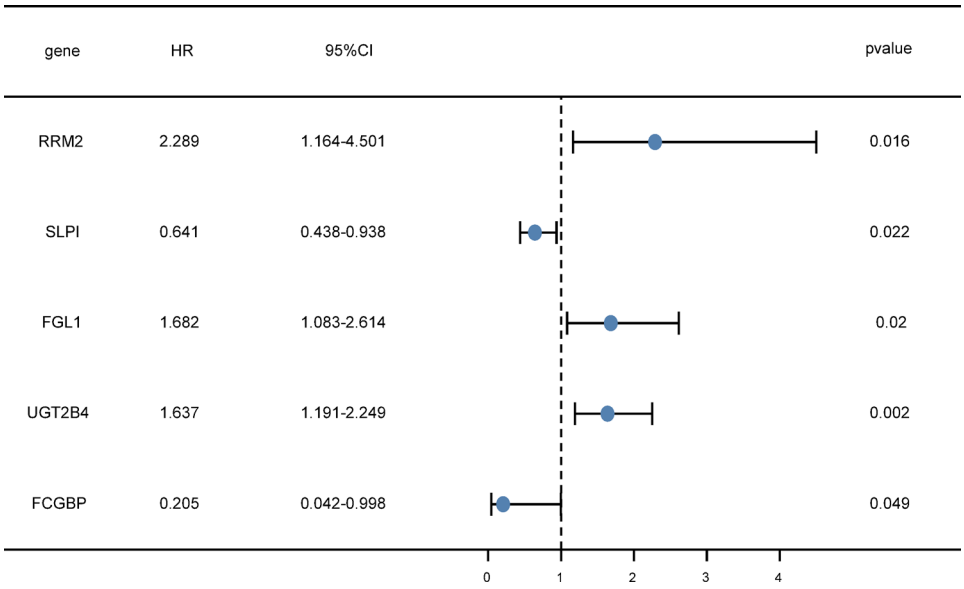

Table 1. 5 genes associated with overall survival (OS) are shown.

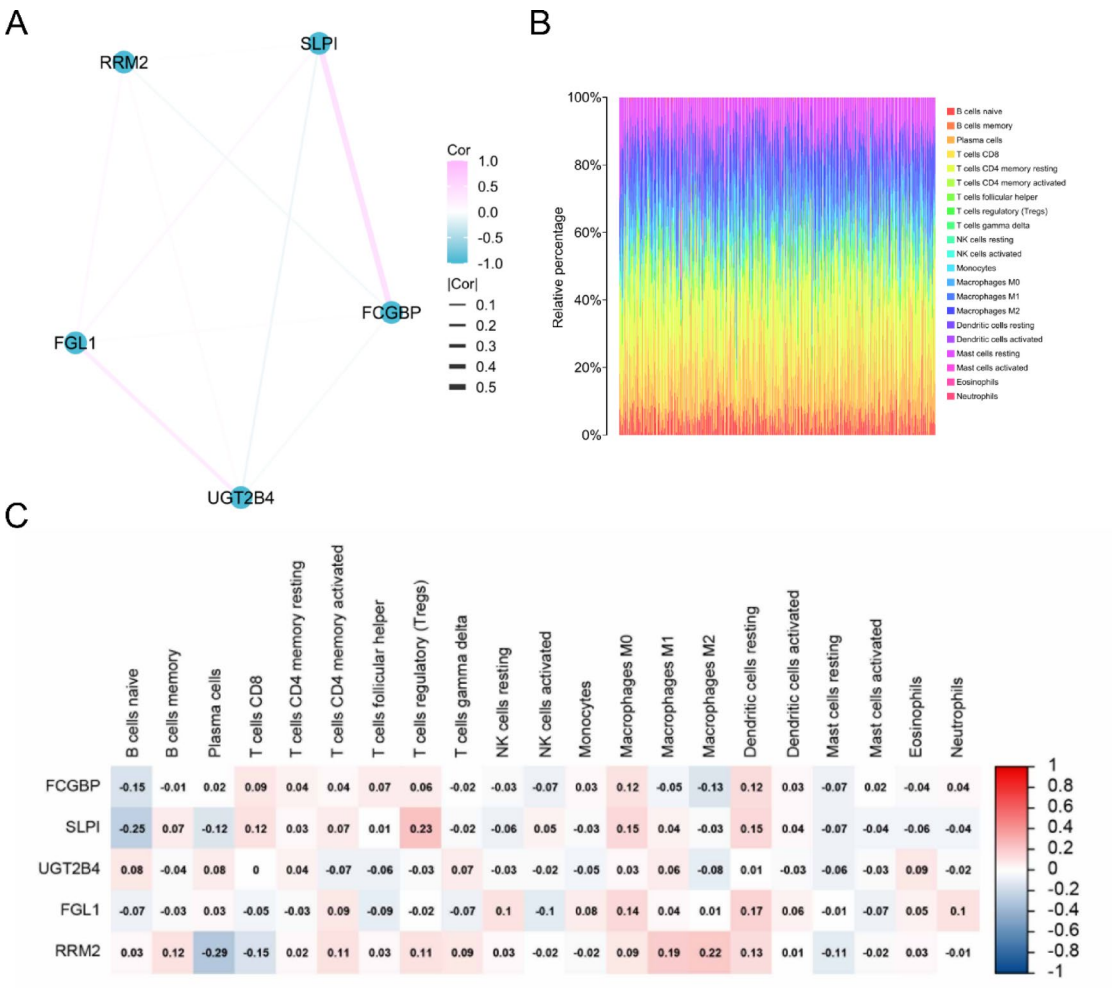

Fig. 2. Five target genes and immune cells: (**A**) The link between the five target genes; (**B**) The relationship between DEGs and immune cells; (**C**) The relationship between five target genes and immune cells.

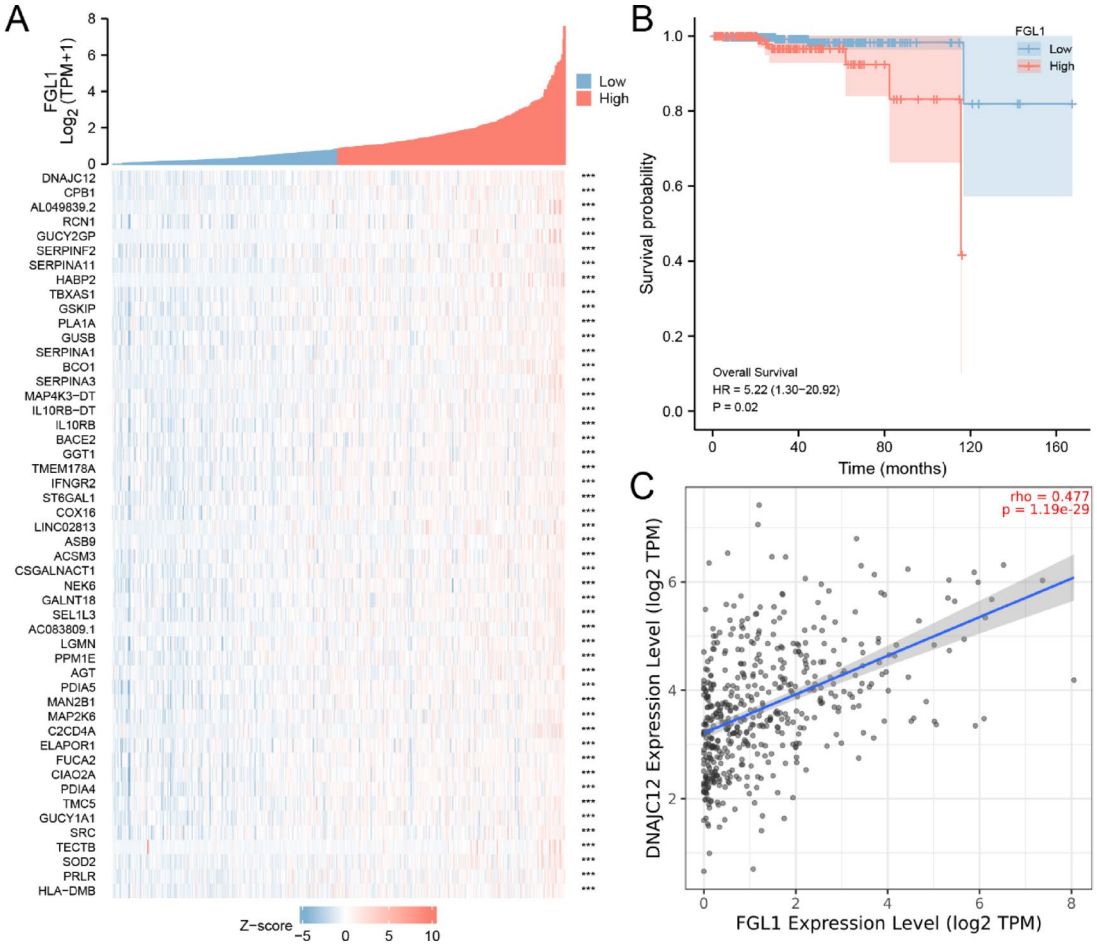

Fig. 3. Expression of FGL1-related genes: (**A**) Heatmap plot of the single-gene difference analysis of FGL1; (**B**) Correlation between FGL1 gene expression and overall survival; (**C**) Correlation between FGL1 and DNAJC12. *** is $P < 0.001$.

Pathway analysis[15] showed that FGL1 and its related genes were not only enriched in Network Map of Sarscov2 Signaling, Nuclear Receptors Meta pathway and Striated Muscle Contraction Pathway, but also involved in the biological processes of platelet and Muscle Contraction (Fig. 4C). In addition, we performed GO/KEGG combined LOGFC analysis (Fig. 4D).

We study the direction of cell death by FGL1-related genes and DNAJC12-related genes. We identified 121 apoptosis-related genes in the Amigo 2 database, and along with the Venn diagram, we identified 54 apoptosis-related genes among FGL1-and DNAJC12-related genes (Fig. S1A,B). Through the String database, we found a link between FGL1 and DNAJC12, possibly through HSPA8 and FN1 (Fig. S1C,D). We analyzed the KEGG pathway of these genes and found that 15 genes were enriched in the apoptotic pathway.

The change of FGL1 expression affects the proliferation and migration of PC3 and DU145 cells

We examined four cell lines of human prostate tumor cells and found that FGL1 was most highly expressed in PC3 (Fig. S2). PC3 cells were used to investigate the effect of FGL1 on pCa. The CCK-8 assay assessed the impact of FGL1 silencing on PC3 cell viability. We found that the silencing of FGL1 significantly inhibited the proliferation of PC3 cells compared with the control group, showing statistically significant differences between the 18 and 24 h (Fig. 5A). The result of ki-67 staining showed that cell proliferation was markedly decreased in the FGL1-siRNA group compared with the control group (Fig. 5B). Transwell experiments showed that the number of cells migrated in FGL1-siRNA group was significantly decreased (Migration Fold change = 0.52) (Fig. 5C,D). Colony formation assay showed that there was no significant difference between Con group and NC Group after 7 days of cell culture, while the number of cells in siFGL1 group decreased significantly (Con Fold change = 0.58; NC-siRNA Fold change = 0.63) (Fig. 5E,F). In addition, the number of DU145 cells overexpressing FGL1 was increased compared with the control group (Fold change = 2.05) (Fig. 5G,H). Scratch assay showed that silencing FGL1 inhibited cell proliferation in PC3 cells (PC3 Fold change = 0.55; PC3-NC Fold change = 0.58) (Fig. 5I,J), while overexpression of FGL1 accelerated cell proliferation in DU145 cells (Fold change = 1.96) (Fig. 5K,L). These results suggest that alterations in FGL1 can affect prostate cancer cell growth.

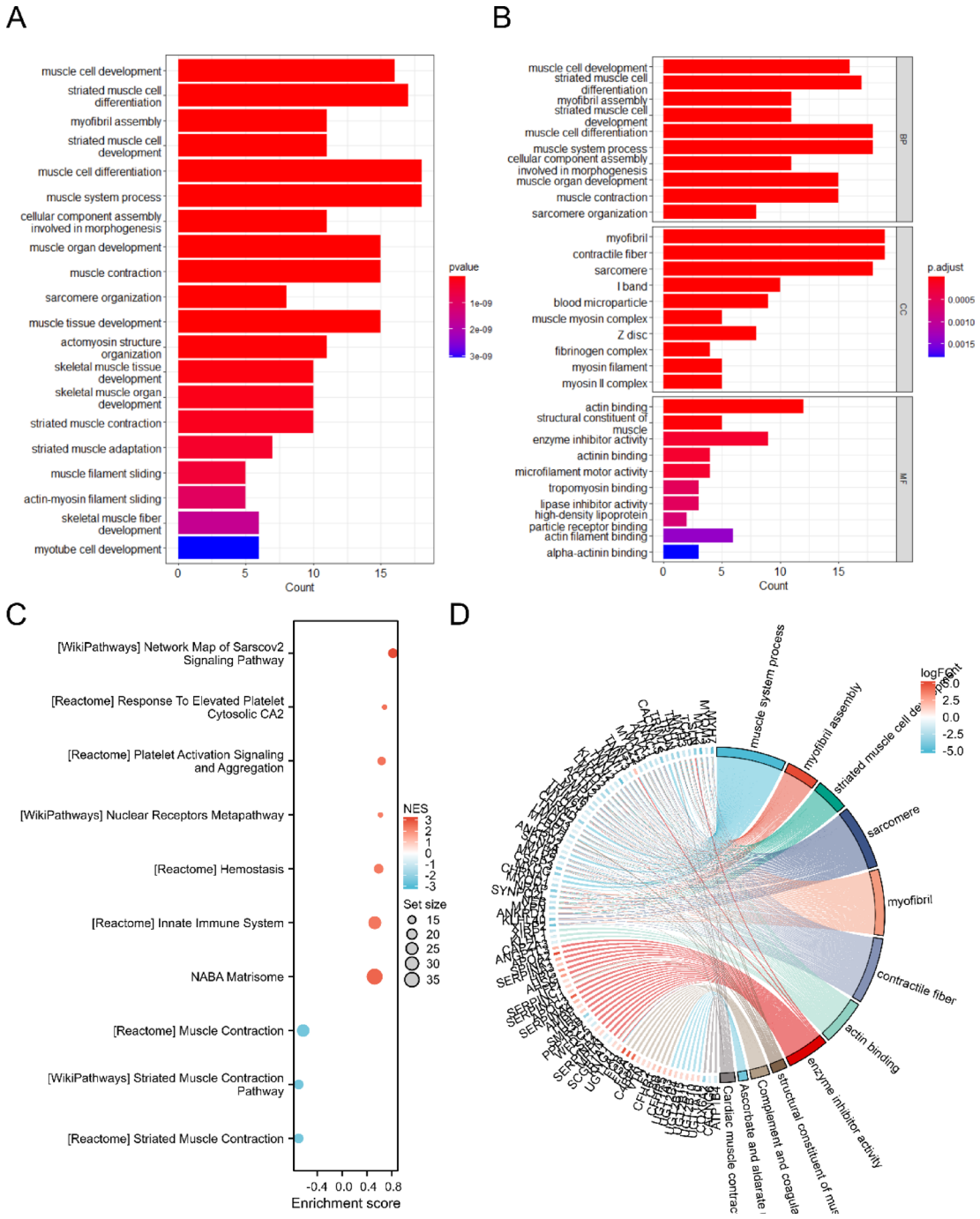

Fig. 4. The interaction network analysis of FGL1-related genes: (**A**, **B**) Gene Ontology (GO) term of FGL1-related genes in PRAD; (**C**) Kyoto Encyclopedia of Genes and Genomes (KEGG) pathway analyses of FGL1-related genes in PRAD; (**D**) GO/KEGG combined LogFC analysis.

FGL1 regulates apoptosis via DNAJC12 in pCa cells

To explore the potential molecular mechanism of FGL1 underlying cell apoptosis, we tested the expression of apoptosis-related genes, such as pro-apoptotic genes cleaved-caspase-3 and the anti-apoptotic gene Bcl-2. Western blotting analysis confirmed that siRNA transfection efficiently reduced FGL1 expression (Con Fold change = 0.34;NC-siRNA Fold change = 0.25). At the same time, the expression of DNAJC12 and BCL-2 was decreased (DNAJC12 Con Fold change = 0.31; DNAJC12 NC-siRNA Fold change = 0.29; BCL-2 Con Fold change = 0.26, BCL-2 NC-siRNA Fold change = 0.25), and the expression of cleaved-caspase-3 was increased (Con Fold change = 1.98; NC-siRNA Fold Change = 1.87) (Fig. 6A,B). The Flow cytometry showed that silencing FGL1 resulted in an increase in apoptosis of PC3 cells by 16% (Fig. 6C,D). Furthermore, overexpression of FGL1 decreased the expression of cleaved-caspase-3 in DU145 cells (Fig. 6E,F).

FGL1 mediates the EMT process via FN1

Previously, we found that FGL1 is associated with DNAJC12 by FN1. We established a tumor xenograft model by subcutaneously injecting PC3 cell lines into immunodeficient mice. By comparing the weight of subcutaneous tumorigenesis, we found that the tumor tissue of the FGL1-siRNA group was significantly smaller than that of the NC-siRNA group (Fold change = 0.35) (Fig. 7A). After silencing FGL1, the expression of FN1, N-cadherin, Vimentin, β-catenin, and E-cadherin decreased, while the expression of E-cadherin increased (Fig. 7B). Furthermore, we verified the expression of EMT markers in DU145 cells overexpressing FGL1. WB results showed that overexpression of FGL1 and E-calcineurin decreased, while N-calcineurin and vimentin increased (Fig. 6E,F).

Discussion

The results suggested that five target genes (RRM2, SLPI, FGL1, UGT2B4, and FCGBP) have diagnostic significance. In addition, we performed correlation analysis on the 5 genes we screened. The results showed that there was a specific relationship between the 5 genes. Subsequently, we performed an analysis of immune cell infiltration. The results showed they were related to many immune cells and cell cycle. We chose FGL1 as the target of the study after searching the relevant literature. FGL1 has been the most potential immune checkpoint target in recent years. Its immunological mechanism in solid tumors such as lung and liver cancers has been revealed[11,16]. However, few studies have reported that FGL1 causes cell death via other mechanisms. Using bioinformatic analysis, we investigated the association of FGL1 with other genes in pCa. To explore the biological function of FGL1, we screened the related genes of FGL1 and performed functional enrichment and pathway analysis. The results showed that FGL1-related genes were related to the growth and development of muscle cells and the morphological changes of muscle systems and organs. It is also involved in cellular processes. We also found that FGL1 and its related genes are involved in the Network Map of Sarscov2 Signaling, Nuclear Receptors Meta Pathway and Striated Muscle Contraction Pathway, the biological processes of platelet and Muscle Contraction. It is worth mentioning that we found that DNAJC12 was the most positively correlated among the FGL1-related genes through a series of analyses. DNAJC12 belongs to the J domain-containing protein of the DnaJ homology C family and represents the heat shock protein subclass[17]. DNAJC12 has a possibly significant effect on lung cancer occurrence by modulating β-catenin activation and expression. DNAJC12 silencing promotes lung cancer cell apoptosis[18]. Li Y et al.[19] also reported that DNAJC12 silencing promotes lung cancer cell apoptosis. However, this phenomenon was not observed in pCa.

Next, we tested this association via cell experiments. In addition to the blank control group, we introduced the NC-siRNA group as another control group for FGL1-siRNA. The grayscale analysis confirmed that FGL1 is highly expressed in pCa cells. We determined that FGL1 was silenced via western blotting. FGL1 silencing inhibited prostate cell proliferation, as demonstrated by CCK-8 and Ki-67. Consistently, we found that DNAJC12 showed a higher expression pattern in pCa tissues and cells and that high expression of DNAJC12 may promote pCa cell growth and inhibited apoptosis. Inhibition of FGL1 reduced DNAJC12 expression, with flow cytometry revealing decreased BCL-2 (anti-apoptotic gene) and increased cleaved-caspase-3 (pro-apoptotic gene) levels. The BCL-2 family regulates apoptosis by balancing anti-apoptotic genes (A1/BCL-2/BCL-XL/Bcl-w/MCL1) and pro-apoptotic genes (BAK/BAX), influencing mitochondrial outer membrane permeabilization (MOMP). This subsequently activates caspase-3 through cytochrome c release, apoptosome formation, and caspase-9/APAF1 signaling[20–22]. FGL1 silencing likely induces prostate cancer (pCa) cell apoptosis via DNAJC12. DNAJC12 promotes tumor growth by regulating β-catenin activation[19,23], and the Wnt/β-catenin pathway modulates apoptosis[24,25], though detailed mechanisms require further investigation. In addition, we found that overexpression of FGL1 decreased the expression of cleaved-caspase-3, which further suggests that changes in FGL1 expression can affect prostate cancer cell apoptosis. When we enriched FGL1-related genes, we found a link between them and muscle cells and their biological processes. The interaction with muscle cells has been documented to promote the progression of prostate cancer[26]. Co-culture of muscle cells with prostate cancer cells promotes tumor cell fusion (forming multinucleated tumor cells) and induces drug resistance, accelerating prostate cancer progression. Notably, actin levels were elevated in the serum of prostate cancer patients after a 12-week exercise intervention and suppressed ADT-treated prostate cancer progression[27]. In a study of 10 prostate cancer patients undergoing a 12-week exercise program, fasting blood was collected pre- and post-intervention. Serum myokines and DU145 prostate cancer cell growth were analyzed. Cells cultured with post-intervention serum exhibited similar growth patterns to baseline serum in the first 24 h, followed by gradual divergence. At 72 h, the cell index decreased by 21.3% (baseline: 5.829 ± 1.112 vs. post-intervention: 4.566 ± 1.515; $P = 0.012$). The mean 72-hour cell growth rate declined by 22.5% (baseline: 0.080 ± 0.016 vs. post-intervention: 0.062 ± 0.021; $P = 0.012$), with significant suppression after 25 h and marked differences post-45 h. Emerging evidence identifies skeletal muscle as an endocrine organ[28]?Many endocrine factors, including myokines, are involved in tumor progression. Our evidence suggests that FGL1 may be involved in the progression of prostate cancer through these pathways.

Epithelial-mesenchymal transition (EMT) involves dynamic changes in the cell tissue from the epithelial to the mesenchymal phenotype, leading to functional changes in cell migration and invasion. During the multi-step progression of initially benign cancers, epithelial cells acquire some distinct mesenchymal features, allowing them to invade adjacent tissues locally and then spread to distant tissues[29]. Through bioinformatics analysis, we found that FGL1 and DNAJC12 were associated with FN1. FN1 participates in a variety of tumor EMT processes[30,31]. Therefore, we examined EMT markers and found that silencing FGL1 decreased the expression of FN1, N-cadherin, and vimentin and increased the expression of E-cadherin. After overexpression of FGL1, the expression of E-calcineurin decreased, while the expression of N-calcineurin and vimentin increased. These results indicate that silencing FGL1 may inhibit the EMT process. In addition, other groups found that high expression of FN1 was positively associated with the progression and metastasis of prostate cancer, which

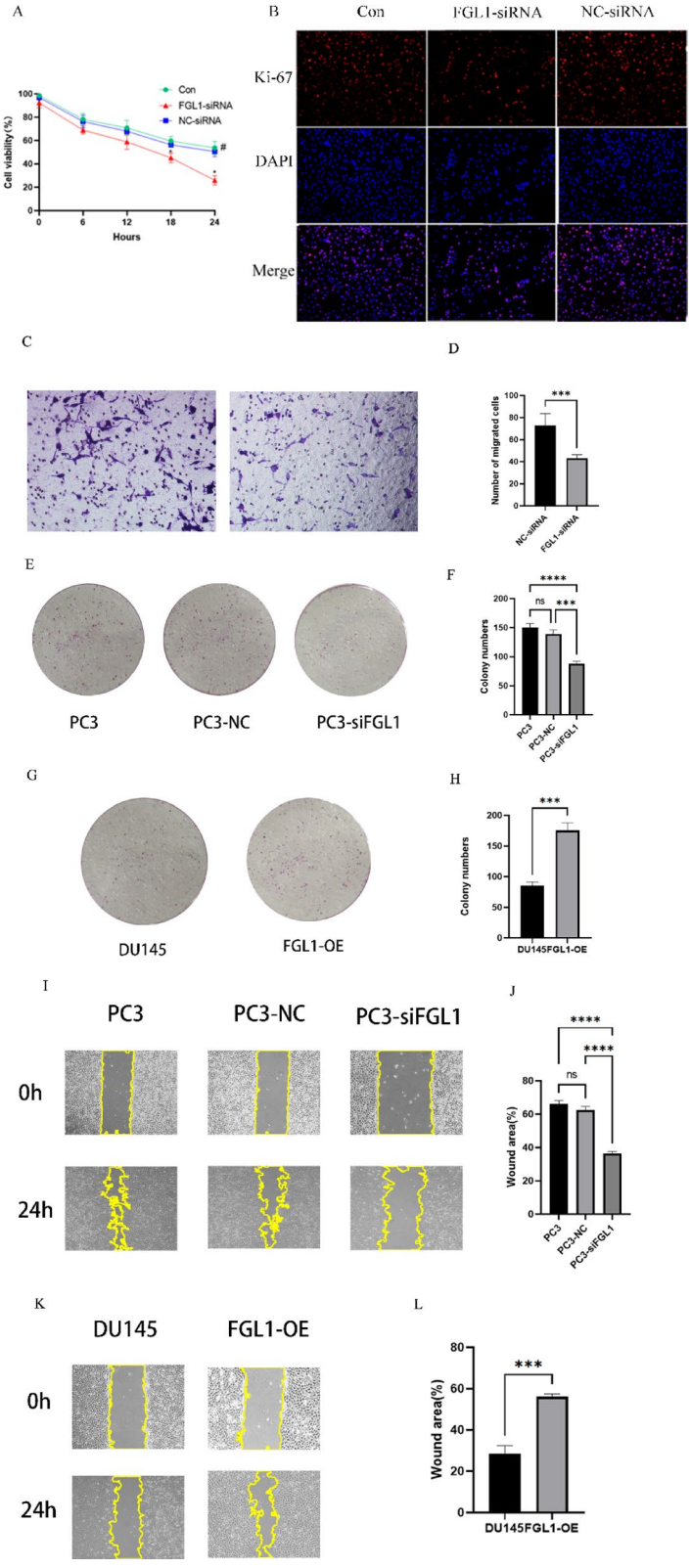

is consistent with our conclusions[32]. It has been found that FGL1 knockdown can significantly inhibit the expression of EMT in head and neck squamous-cell carcinoma carcinoma (HNSCC)[33]. In addition, it has been found that overexpression of FGL1 enhances cell migration, invasion and metastasis of renal cell carcinoma by activating EMT[34]. The prognosis of patients with high expression of FGL1 in tumor tissue was worse in gastric and hepatocellular carcinoma, and we initially found consistent results in prostate cancer[35,36].The role of the Wnt/β-catenin pathway in tumors has been revealed and is widely present in multiple tumors[37]. In canonical Wnt signaling, it leads to the phosphorylation of β-catenin by the destruction complex. In this state, β-catenin is phosphorylated by GSK3β, ubiquitinated by β-TrCP200 and targeted for proteasomal degradation[38]. Without

◀**Fig. 5**. FGL1 silencing inhibits PCa cell proliferation and migration. (**A**) The proliferation of PC3 cells was inhibited after FGL1 silencing as measured by CCK-8. * Compared with Con group or NC-siRNA Group, FGL1-siRNA group showed significant difference ($p < 0.05$); # The comparison of Con Group and NC-siRNA Group was $P > 0.05$. (**B**) Ki-67 detected PC3 cell proliferation percentage after silencing FGL1: The proliferation rate of PC3 cells decreased after silencing FGL1. (**C**) Representative results of silencing FGL1 on PC3 cell migration (**D**) Statistical analysis of the effect of silencing FGL1 on the migration of PC3 cells. (**E**) silencing FGL1 in PC3 cell lines inhibited cell proliferation (**F**) statistical analysis of colony formation experiments in PC3 cell lines (**G**) overexpression of FGL1 in DU145 cell lines promoted cell growth (**H**) statistical analysis of colony formation experiments in DU145 cell lines (**I**) silencing FGL1 in PC3 cell lines inhibited cell migration (**J**) statistical analysis of scratch experiments in PC3 cell lines (**K**) overexpression of FGL1 in DU145 cell lines promoted cell migration (**L**) statistical analysis of DU145 cell line scratch assay. *Con* blank control group, *NC-siRNA* negative control group, *FGL1-siRNA* FGL1 silencing group, *PC3* PC3 cell line blank control group, *PC3-NC* PC3 cell line negative control group, *PC3-siFGL1* FGL1 silencing group in PC3 cell line, *DU145* DU145 cell line blank control group, *FGL1-OE* FGL1 overexpression group in DU145 cell line. ns $P > 0.05$, $^{*}P < 0.05$, $^{**}P < 0.01$, $^{****}P < 0.001$.

nuclear β-catenin, a repressive complex containing TCF/LEF and transducing-like enhancer protein recruits HDACs to repress target genes. We examined the expression of β-catenin in nude mouse tumors and showed that the expression of β-catenin was decreased after silencing FGL1. This suggests that silencing FGL1 may inhibit the Wnt/β-catenin signaling pathway, which delays tumor progression. We examined the expression of β-catenin in nude mouse tumors and showed that the expression of β-catenin was decreased after silencing FGL1. This suggests that silencing FGL1 may inhibit the Wnt/β-catenin signaling pathway. The above experiments indicate that FGL1 may affect EMT progression and the Wnt/β-catenin signaling pathway via DNAJC12, thereby delaying the progression of prostate cancer. Unfortunately, we have no evidence of a direct link between FGL1 and DNAJC12, and we may further elucidate the relationship between the two by co-immunoprecipitation experiments in the future.

FGL1 has been shown to have an immunosuppressive effect in other tumors[13,17,22,39,40]; however, this was not investigated in this study. We are already preparing new experiments to explore the immune role of FGL1 in pCa. Nevertheless, FGL's immune function in pCa needs further study. In recent years, pCa gene-related targeted therapy has made good progress. Statistically, these genes include mismatch repair (MMR) genes (MLH1, MSH2, MSH6, and PMS2) and homologous recombination genes (BRCA1/2, ATM, PALB2, Chek2)[41]. Through our experiments, We found that silencing FGL1 inhibited tumor growth in mice, suggesting that FGL1 is involved in tumor progression, and blocking the expression of this gene may delay tumor progression; This provides a new direction for the clinical development of drugs for the treatment of prostate cancer.

Collectively, our findings demonstrate that silencing FGL1 inhibits prostate cancer cell proliferation and promotes apoptosis. Furthermore, FGL1 may regulate the Wnt signaling pathway and EMT, as evidenced by our experimental data. Importantly, in vivo studies using a CDX model revealed that FGL1 knockdown significantly delays tumor progression. Although FGL1—a primary ligand of LAG-3—has recently emerged as a potential immunotherapeutic target in solid tumors, the low immunogenicity of prostate cancer has limited the efficacy of current immunotherapies in this context. Notably, our study provides the evidence of FGL's involvement in prostate cancer progression independent of its immune-related functions. Future research should focus on elucidating the interplay between FGL1 and the tumor microenvironment, immune checkpoints (e.g., LAG-3/PD-1), and cancer cell metabolic reprogramming. These investigations could further unravel FGL's multifaceted roles in prostate carcinogenesis and provide a theoretical foundation for developing targeted therapies.

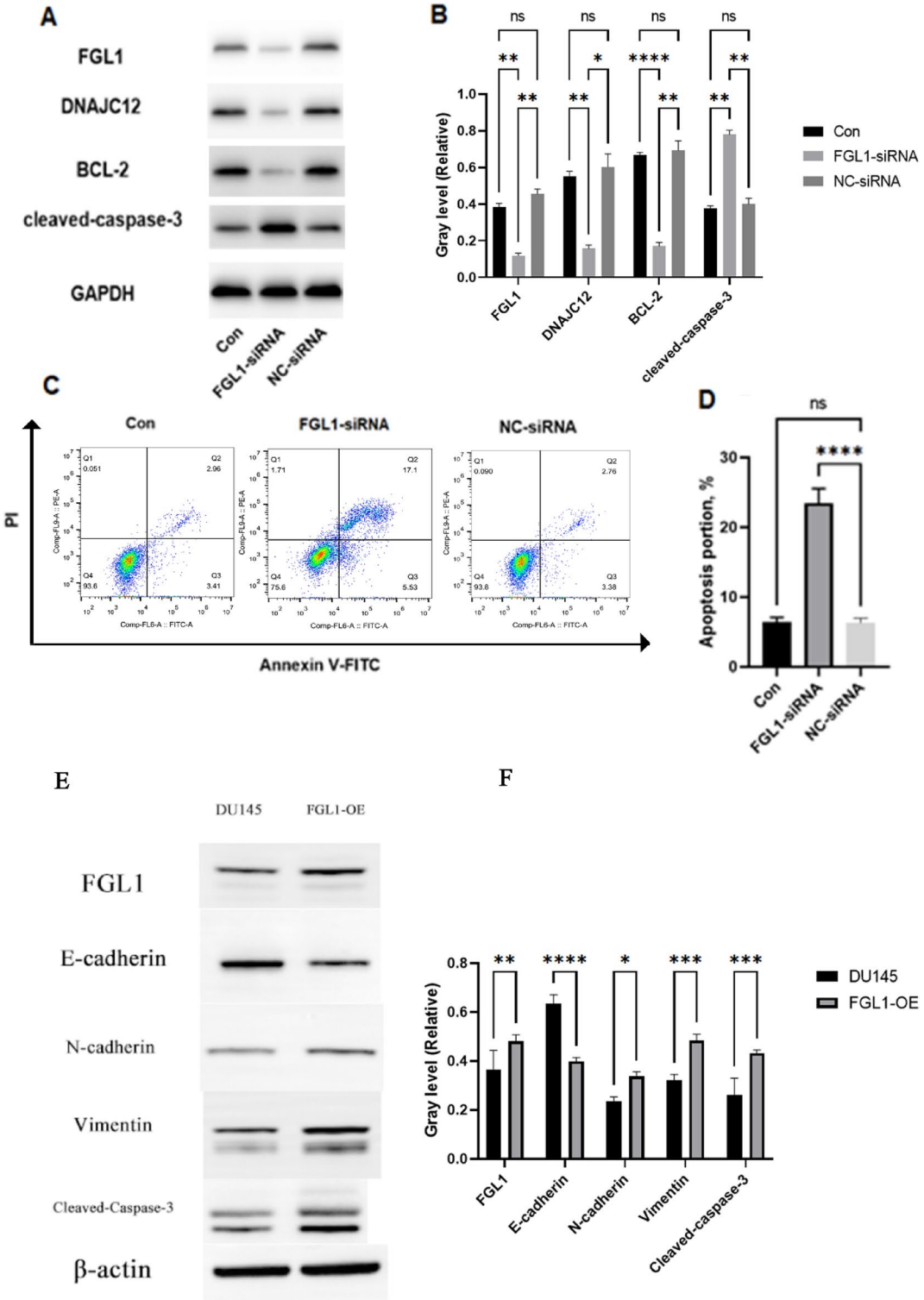

Fig. 6. FGL1 regulates apoptosis via DNAJC12 in PCa cells. (**A**, **B**) Western blot analysis was applied to determine the effect of FGL1 on DNAJC12, BCL-2, and cleaved-caspase-3 in the PC3 cell line. (**C**, **D**) Flow cytometry detection of PC3 cell apoptosis after transfection: The apoptosis rate of PC3 cells was increased after silencing FGL1. (**E**, **F**) Western blot analysis was applied to determine the effect of FGL1 on E-cadherin, N-cadherin, Vimentin and cleaved-caspase-3 in the DU145 cell line. *Con* blank control group, *NC-siRNA* negative control group, *FGL1-siRNA* FGL1 silencing group, *DU145* DU145 cell line blank control group, *FGL1-OE* FGL1 overexpression group in DU145 cell line. Ns $P > 0.05$, $^{*}P < 0.05$, $^{**}P < 0.01$, $^{****}P < 0.001$.

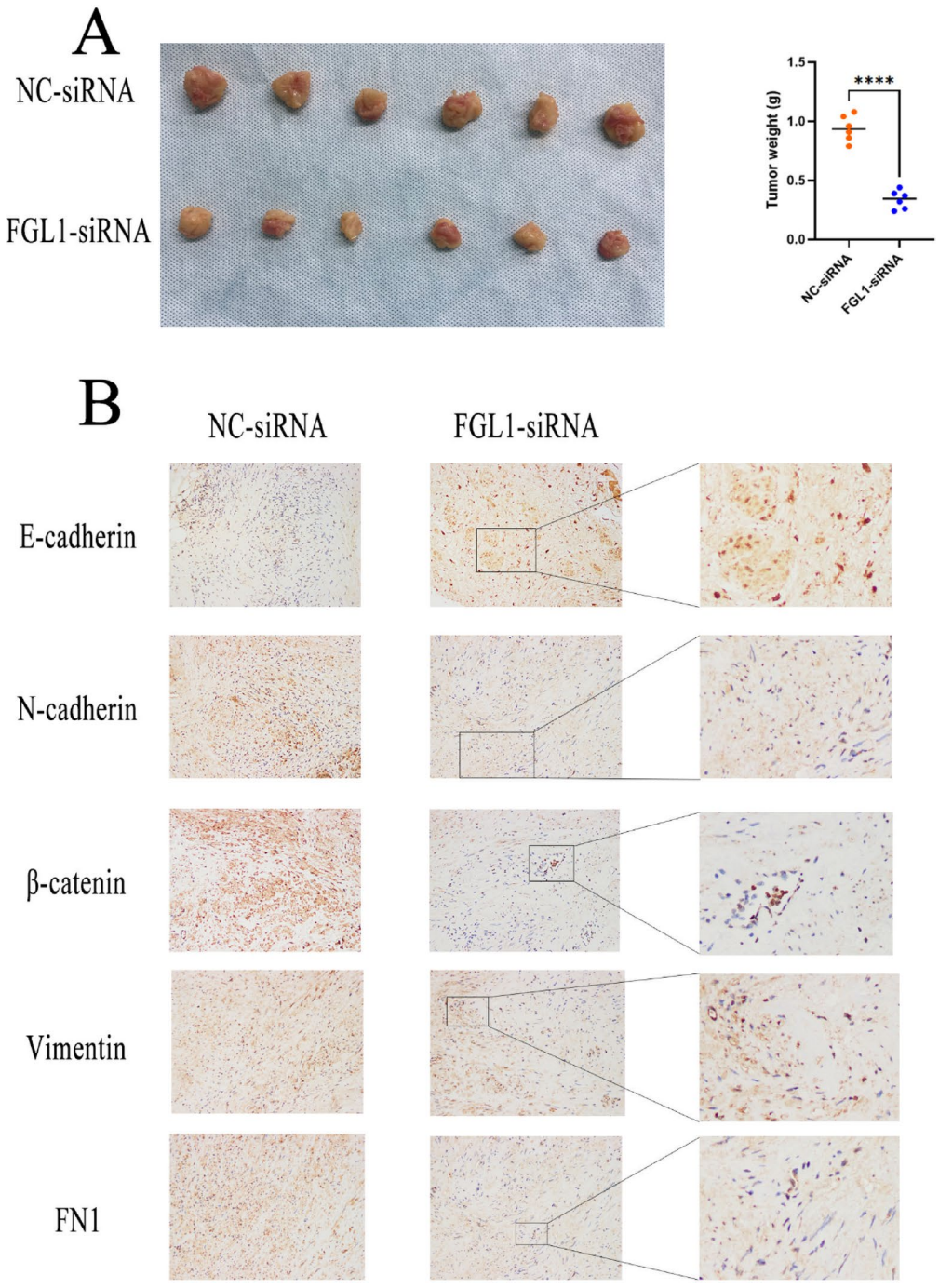

Fig. 7. Silencing FGL1 inhibits tumor growth in xenograft mice. (**A**) Mice received xenografts of PC3 cell line tumors by subcutaneous injection. After 4 weeks of subcutaneous injection, xenograft tumors were removed and measured. (**B**) The expression of FN1, β-catenin and EMT markers in xenograft tumors of mice was detected by immunohistochemistry. *NC-siRNA* negative control group, *FGL1-siRNA* FGL1 silencing group. ****$P < 0.001$.

Data availability

The datasets used in this research are available in the following public databases: TCGA (https://portal.gdc.cancer.gov/), TIMER2.0 (http://timer.cistrome.org/), AmiGO 2(https://amigo.geneontology.org/amigo/search/bioentity? q=apoptosis). In addition to datasets from public databases, other datasets used and analyzed during the present study are available from the corresponding author on reasonable request. Some or all data, models, or codes that support the findings of this study are available from the corresponding author upon reasonable request.

Received: 19 October 2024; Accepted: 28 May 2025
Published online: 06 June 2025

References

1. Bray, F. et al. Global cancer statistics 2018: GLOBOCAN estimates of incidence and mortality worldwide for 36 cancers in 185 countries. *Cancer J. Clin.* **68** (6), 394–424. https://doi.org/10.3322/caac.21492 (2018).
2. Siegel, R. L., Miller, K. D. & Jemal, A. Cancer statistics, 2019. *Cancer J. Clin.* **69** (1), 7–34. https://doi.org/10.3322/caac.21551 (2019).
3. Khusbu, F. Y. et al. Resveratrol induces depletion of TRAF6 and suppresses prostate cancer cell proliferation and migration. *Int. J. Biochem. Cell Biol.* **118**, 105644. https://doi.org/10.1016/j.biocel.2019.105644 (2020).
4. Wang, G., Zhao, D., Spring, D. J. & DePinho, R. A. Genetics and biology of:prostate cancer. *Genes Dev.* **32** (17–18), 1105–1140. https://doi.org/10.1101/gad.315739.118 (2018).
5. Rebello, R. J. et al. Prostate cancer. *Nat. Reviews Disease Primers.* **7** (1), 9. https://doi.org/10.1038/s41572-020-00243-0 (2021).
6. Cornford, P. et al. EAU-ESTRO-SIOG guidelines on prostate cancer. Part II: treatment of relapsing, metastatic, and Castration-Resistant prostate Cancer. *Eur. Urol.* **71** (4), 630–642. https://doi.org/10.1016/j.eururo.2016.08.002 (2017).
7. Sweeney, C. J. et al. Chemohormonal therapy in metastatic Hormone-Sensitive prostate Cancer. *N. Engl. J. Med.* **373** (8), 737–746. https://doi.org/10.1056/NEJMoa1503747 (2015).
8. Teo, M. Y., Rathkopf, D. E. & Kantoff, P. Treatment of advanced prostate Cancer. *Annu. Rev. Med.* **70**, 479–499. https://doi.org/10.1146/annurev-med-051517-011947 (2019).
9. Parker, C. et al. &. Electronic address: clinicalguidelines@esmo.org Prostate cancer: ESMO clinical practice guidelines for diagnosis, treatment and follow-up. *Ann. Oncol. Off. J. Eur. Soc. Med. Oncol.* **31** (9), 1119–1134. https://doi.org/10.1016/j.annonc.2020.06.011 (2020).
10. Chan, K. Y. et al. Positional expression profiling indicates candidate genes in deletion hotspots of hepatocellular carcinoma. *Mod. Pathology: Official J. United States Can. Acad. Pathol. Inc.* **19** (12), 1546–1554. https://doi.org/10.1038/modpathol.3800674 (2006).
11. Nayeb-Hashemi, H. et al. Targeted disruption of fibrinogen like protein-1 accelerates hepatocellular carcinoma development. *Biochem. Biophys. Res. Commun.* **465** (2), 167–173. https://doi.org/10.1016/j.bbrc.2015.07.078 (2015).
12. Wang, J., Sanmamed, M. F., Datar, I., Su, T. T., Ji, L., Sun, J., Chen, L., Chen,Y., Zhu, G., Yin, W., Zheng, L., Zhou, T., Badri, T., Yao, S., Zhu, S., Boto, A.,Sznol, M., Melero, I., Vignali, D. A. A., Schalper, K., … Chen, L. Fibrinogen-like protein 1 Is a major immune inhibitory ligand of LAG-3. *Cell* **176** (1–2), 334–347.e12. (2019).
13. Qian, W., Zhao, M., Wang, R. & Li, H. Fibrinogen-like protein 1 (FGL1): the next immune checkpoint target. *J. Hematol. Oncol.* **14** (1), 147. https://doi.org/10.1186/s13045-021-01161-8 (2021).
14. Kgatle, M. M. et al. Immune checkpoints, inhibitors and radionuclides in prostate cancer: promising combinatorial therapy approach. *Int. J. Mol. Sci.* **22** (8), 4109. https://doi.org/10.3390/ijms22084109 (2021).
15. Kanehisa, M. Toward understanding the origin and evolution of cellular organisms. *Protein Sci.* **28**(11), 1947–1951. https://doi.org/10.1002/pro.3715 (2019).
16. Lehtiö, J., Arslan, T., Siavelis, I., Pan, Y., Socciarelli, F., Berkovska, O., Umer,H. M., Mermelekas, G., Pirmoradian, M., Jönsson, M., Brunnström, H., Brustugun, O.T., Purohit, K. P., Cunningham, R., Foroughi Asl, H., Isaksson, S., Arbajian, E.,Aine, M., Karlsson, A., Kotevska, M., … Orre, L. M. Proteogenomics of non-small cell lung cancer reveals molecular subtypes associated with specific therapeutic targets and immune evasion mechanisms. *Nat. Cancer* **2** (11), 1224–1242. (2021).
17. Sun, C., Gao, W., Liu, J., Cheng, H. & Hao, J. FGL1 regulates acquired resistance to gefitinib by inhibiting apoptosis in non-small cell lung cancer. *Respir. Res.* **21** (1), 210. https://doi.org/10.1186/s12931-020-01477-y (2020).
18. Roosen, D. A., Blauwendraat, C., Cookson, M. R. & Lewis, P. A. DNAJC proteins and pathways to parkinsonism. *FEBS J.* **286** (16), 3080–3094. https://doi.org/10.1111/febs.14936 (2019).
19. Li, Y. et al. DNAJC12 promotes lung cancer growth by regulating the activation of βcatenin. *Int. J. Mol. Med.* **47** (6), 105. https://doi.org/10.3892/ijmm.2021.4938 (2021).
20. Carneiro, B. A. & El-Deiry, W. S. Targeting apoptosis in cancer therapy. *Nat. Rev. Clin. Oncol.* **17** (7), 395–417. https://doi.org/10.1038/s41571-020-0341-y (2020).
21. Jin, Z. & El-Deiry, W. S. Overview of cell death signaling pathways. *Cancer Biol. Ther.* **4** (2), 139–163. https://doi.org/10.4161/cbt.4.2.1508 (2005).
22. Yao, C. et al. Boschniakia Rossica polysaccharide triggers laryngeal carcinoma cell apoptosis by regulating expression of Bcl-2, Caspase-3, and P53. *Med. Sci. Monitor: Int. Med. J. Experimental Clin. Res.* **23**, 2059–2064. https://doi.org/10.12659/msm.901381 (2017).
23. Wang, J., Huang, H. & Liu, F. *DNAJC12* activated by *HNF1A* enhances aerobic Glycolysis and drug resistance in non-small cell lung cancer. *Annals Translational Med.* **10** (8), 492. https://doi.org/10.21037/atm-22-1475 (2022).
24. Chu, C. W. et al. Thioridazine enhances P62-Mediated autophagy and apoptosis through Wnt/β-Catenin signaling pathway in glioma cells. *Int. J. Mol. Sci.* **20** (3), 473. https://doi.org/10.3390/ijms20030473 (2019).
25. Sha, L., Ma, D. & Chen, C. Exosome-mediated Hic-5 regulates proliferation and apoptosis of osteosarcoma via Wnt/β-catenin signal pathway. *Aging* **12** (23), 23598–23608. https://doi.org/10.18632/aging.103546 (2020).
26. Uygur, B. et al. Interactions with muscle cells boost fusion, stemness, and drug resistance of prostate Cancer cells. *Mol. cancer Research: MCR.* **17** (3), 806–820. https://doi.org/10.1158/1541-7786.MCR-18-0500 (2019).
27. Kim, J. S. et al. Myokine expression and Tumor-Suppressive effect of serum after 12 Wk of exercise in prostate Cancer patients on ADT. *Med. Sci. Sports. Exerc.* **54** (2), 197–205. https://doi.org/10.1249/MSS.0000000000002783 (2022).
28. Hoffmann, C. & Weigert, C. Skeletal muscle as an endocrine organ: the role of myokines in exercise adaptations. *Cold Spring Harbor Perspect. Med.* **7** (11), a029793. https://doi.org/10.1101/cshperspect.a029793 (2017).
29. Yang, J., Antin, P., Berx, G., Blanpain, C., Brabletz, T., Bronner, M., Campbell,K., Cano, A., Casanova, J., Christofori, G., Dedhar, S., Derynck, R., Ford, H. L.,Fuxe, J., García de Herreros, A., Goodall, G. J., Hadjantonakis, A. K., Huang, R.Y. J., Kalcheim, C., Kalluri, R., … EMT International Association (TEMTIA). Guidelines and definitions for research on epithelial-mesenchymal transition. *Nat. Rev. Mol. Cell Biol.* **21** (6), 341–352. (2020).
30. Zhang, X. et al. MACC1 promotes pancreatic cancer metastasis by interacting with the EMT regulator SNAI1. *Cell Death Dis.* **13** (11), 923. https://doi.org/10.1038/s41419-022-05285-8 (2022).
31. Hajimehdipoor, H., Tahmasvand, Z., Nejad, F. G., Maresca, M. & Rajabi, S. Rutin promotes proliferation and orchestrates Epithelial-Mesenchymal transition and angiogenesis in MCF-7 and MDA-MB-231 breast Cancer cells. *Nutrients* **15** (13), 2884. https://doi.org/10.3390/nu15132884 (2023).
32. Li, X. F., Selli, C., Zhou, H. L., Cao, J., Wu, S., Ma, R. Y., Lu, Y., Zhang, C. B.,Xun, B., Lam, A. D., Pang, X. C., Fernando, A., Zhang, Z., Unciti-Broceta, A., Carragher,N. O., Ramachandran, P., Henderson, N. C., Sun, L. L., Hu, H. Y., Li, G. B., … Qian,B. Z. Macrophages promote anti-androgen resistance in prostate cancer bone disease.*J. Exp. Med.* **220** (4), e20221007. (2023).
33. Pan, Z. et al. Increased FGL1 expression predicts poor prognosis and promotes EMT in head and neck squamous cell carcinoma. *Biochem. Genet.* **62** (3), 2066–2081. https://doi.org/10.1007/s10528-023-10545-z (2024).
34. Lv, Z. et al. FGL1 as a novel mediator and biomarker of malignant progression in clear cell renal cell carcinoma. *Front. Oncol.* **11**, 756843. https://doi.org/10.3389/fonc.2021.756843 (2021).

35. Zhang, Y., Qiao, H. X., Zhou, Y. T., Hong, L. & Chen, J. H. Fibrinogen–like–protein 1 promotes the invasion and metastasis of gastric cancer and is associated with poor prognosis. *Mol. Med. Rep.* **18** (2), 1465–1472. https://doi.org/10.3892/mmr.2018.9097 (2018).
36. Yan, Q. et al. Immune checkpoint FGL1 expression of Circulating tumor cells is associated with poor survival in curatively resected hepatocellular carcinoma. *Front. Oncol.* **12**, 810269. https://doi.org/10.3389/fonc.2022.810269 (2022).
37. Zhan, T., Rindtorff, N. & Boutros, M. Wnt signaling in cancer. *Oncogene* **36** (11), 1461–1473. https://doi.org/10.1038/onc.2016.304 (2017).
38. Latres, E., Chiaur, D. S. & Pagano, M. The human F box protein beta-Trcp associates with the Cul1/Skp1 complex and regulates the stability of beta-catenin. *Oncogene* **18** (4), 849–854. https://doi.org/10.1038/sj.onc.1202653 (1999).
39. Guo, M. et al. Expression and clinical significance of LAG-3, FGL1, PD-L1 and $CD8^+$T cells in hepatocellular carcinoma using multiplex quantitative analysis. *J. Translational Med.* **18** (1), 306. https://doi.org/10.1186/s12967-020-02469-8 (2020).
40. Wang, Y. et al. tRNA-derived fragment tRF-Glu49 inhibits cell proliferation, migration and invasion in cervical cancer by targeting FGL1. *Oncol. Lett.* **24** (4), 334. https://doi.org/10.3892/ol.2022.13455 (2022).
41. Vietri, M. T. et al. Hereditary prostate cancer: genes related, target therapy and prevention. *Int. J. Mol. Sci.* **22** (7), 3753. https://doi.org/10.3390/ijms22073753 (2021).

Acknowledgements
I'm grateful to Professor Peng Wang for introducing Miss Lei Fan to me during the manuscript's completion. Finally thanks to my wife Lei Fan.

Author contributions
SZZ, CCX and HZ made a substantial contribution to the concept or design of the article. SZZ and ZSK drafted the article. SZZ, CCX, LW, YZ and ZSK conducted the experiments and analyzed the data. CCX, LW, JXZ and HZ revised it critically for important intellectual content. JXZ modified the language of this article to make it more readable.All authors reviewed the manuscript.

Funding
This work was funded by the Qingdao Key Medical and Health Discipline Project, the Natural Science Foundation of Shandong Province (No. ZR2023MH327) and the Natural Science Foundation of Qingdao Municipality (No. 23-2-1-193-zyyd-jch).

Declarations

Competing interests
The authors declare no competing interests.

Ethics approval and consent to participate
The Ethics Committee of the Qingdao Municipal Hospital affiliated with Qingdao University and Qingdao University approved this research.

Additional information
Supplementary Information The online version contains supplementary material available at https://doi.org/10.1038/s41598-025-04717-7.

Correspondence and requests for materials should be addressed to H.Z.

Reprints and permissions information is available at www.nature.com/reprints.

Publisher's note Springer Nature remains neutral with regard to jurisdictional claims in published maps and institutional affiliations.